Heliyon 10 (2024) e34659

Contents lists available at ScienceDirect

Heliyon

journal homepage: www.cell.com/heliyon

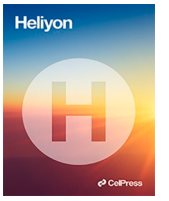

Research article

Phosphorus recovery from ultrafiltered membrane wastewater by biochar adsorption columns: The effect of loading rates

Sofia Maria Muscarella [a], Daniele Di Trapani [b], Vito Armando Laudicina [a], Giorgio Mannina [b,*]

[a] Department of Agricultural, Food and Forest Sciences, University of Palermo, Viale delle Scienze, Building 4, 90128, Palermo, Italy
[b] Department of Engineering, University of Palermo, Viale delle Scienze, Building 8, 90128, Palermo, Italy

ARTICLE INFO

Keywords:
Bench-scale study
Resource recovery
Nutrients removal
Circular economy

ABSTRACT

The present study used bench scale columns filled with biochar for phosphorous (P) recovery from real ultrafiltered wastewater. No studies are available about the potentiality of biochar using ultrafiltered real wastewater. Therefore, this study aimed to assess phosphate (PO_4^{3-}) recovery by biochar-packed columns employing real treated wastewater from an ultrafiltration process. Three flow rates were tested, specifically 0.7, 1.7 and 2.3 L h^{-1}, to gain insights into the optimal working conditions. Results revealed that the maximum amount of PO_4^{3-} recovery (namely, 3.43 mg g^{-1} biochar) can be achieved after 7 h by employing the highest tested flow rate. Furthermore, the phosphorus exchange capacity (PEC) was inversely correlated with the feeding flow rate (FFR), with PEC values equal to 35, 25 and 9 % for FFR of 0.67, 1.7 and 2.3 L h^{-1}, respectively. The pseudo-first order model best approximated the adsorption kinetics, thus suggesting that the adsorption of phosphate by biochar depends on its concentrations (i.e. physiosorption mechanism).

1. Introduction

Phosphorus (P) is essential for plant growth and agricultural productivity [1]. However, being a non-renewable resource, P is continuously extracted from minerals [2]. Several technologies have been developed to remove and recover P from wastewater [3,4]. Among them, the P recovery from water and wastewater by physicochemical adsorption can be an attractive and effective solution, which limits P release into the environment [2].

During the last decade, biochar has been increasingly employed as an adsorbent to remove phosphate (PO_4^{3-}) from aqueous solution Nobaharan et al., 2021; [5]. The physicochemical properties of biochar, such as porous structure, stability, high surface area, pH buffering capacity, and ion-exchange ability, make it a cost-effective and environmentally friendly adsorbent Almanassra et al., 2021; [6,7]. Moreover, biochar is knowingly used as a soil amendment since it can enhance soil carbon sequestration and improve soil physicochemical properties such as reduction of bulk density, enhancement of water-holding capacity and nutrient retention stabilisation of soil organic matter, improvement of microbial activities, and heavy-metal immobilisation [8–10]. Consequently, once enriched with P, biochar could be directly used in soil, acting as a slow-release fertiliser within a circular economy perspective Mannina et al., 2021a.

* Corresponding author. Engineering Department, University of Palermo, Viale delle Scienze, Building 8, 90128 Palermo, Italy.
E-mail address: giorgio.mannina@unipa.it (G. Mannina).

https://doi.org/10.1016/j.heliyon.2024.e34659
Received 23 October 2023; Received in revised form 7 June 2024; Accepted 14 July 2024
Available online 16 July 2024
2405-8440/© 2024 Published by Elsevier Ltd. This is an open access article under the CC BY-NC-ND license (http://creativecommons.org/licenses/by-nc-nd/4.0/).

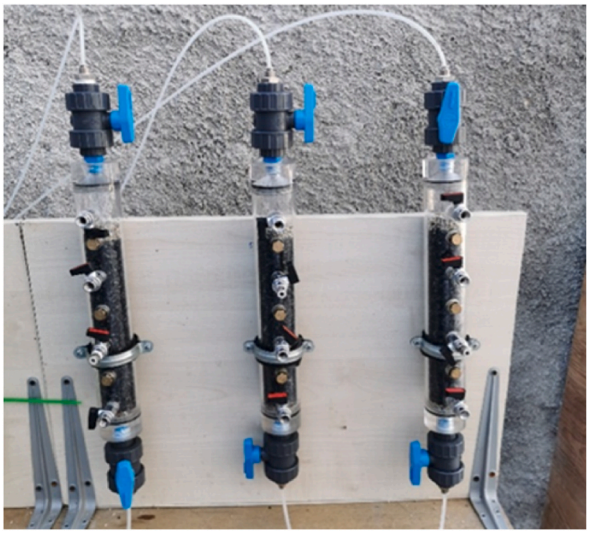

Fig. 1. Biochar packed columns for phosphate (PO_4^{3-}) adsorption from ultrafiltered treated real wastewater.

Almanassra et al. [11] reported that biochar has an adsorption capacity ranging from 7.6 to 303 mg P g^{-1}, depending on the feedstock used for biochar preparation and pyrolysis conditions. However, the ability of biochar to adsorb P depends on many other factors, such as experimental conditions, pH, temperature, P loading rate, biochar dosage, etc [12,13]. Huggins et al. [14] investigated biochar P adsorption capacity in batch and column tests and found a capacity ranging from 2 to 0.8 mg P g^{-1} for batch study and column test, respectively. In a column study, Jung et al. [12] observed that P adsorption on biochar decreases with increasing flow rate, which could be due to insufficient solute residence time to ensure contact between the PO_4^{3-} and the available binding sites. However, most of the studies carried out up to now on P removal are lab-scale experiments employing synthetic water with a spiked solution of salts or phosphoric acid Almanassra et al., 2021, which cannot reflect the complex nature of real wastewater [13]. Only few studies have been conducted with real untreated/treated wastewater [14,15]. Such studies have highlighted several issues related to the competition between PO_4^{3-} and other contaminants on the active adsorption sites, the interaction between PO_4^{3-} and other matters found in the actual streams and the potential blockage of adsorbent pores by biological and organic contaminants [14,15].

Advanced treatment of real wastewater, like membrane bioreactor (MBR) processes or final effluent ultrafiltration, might allow almost complete removal of suspended particles Jupp et al., 2021 and very high removal of pathogen microorganisms such as *Cryptosporidium, Giardia* as well as bacteria, viruses, and parasites [16]. Only few studies have employed unmodified biochar as adsorbent for P removal and recovery from real wastewater at pilot scale plant [17,18]. Recently, Shakoor et al. [19] highlighted the need for studies to evaluate nutrient (P or N) removal and recovery from wastewater by biochar in column systems.

As far as authors are aware, studies have yet to be conducted to assess biochar's ability to recover P from treated real wastewater by advanced treatments (e.g., ultrafiltration membrane). Therefore, studies are needed to address the above-raised issues and establish if real treated wastewater can be a potential source of P instead of pristine biochar. In addition, P adsorption by biochar was investigated by adsorption kinetics studies to determine the time required for the adsorbate to reach maximum adsorption capacity on the adsorbent and the main adsorption mechanism. To our best knowledge, P adsorption kinetic studies on biochar have been only carried out on data obtained from batch tests [12,20,21].

In light of the above, this study aims to investigate the recovery of P by biochar from real wastewater treated with an advanced system (i.e. an ultrafiltration membrane) and its potential mechanism. To test the feasibility of P recovery and assess the role of the feeding flow rate, three different increasing flow rates were tested to determine how the column feed rate could influence the contact time and adsorption of P on biochar. The effects on the maximum amount of PO_4^{3-} recovery, Phosphorus Exchange Capacity (PEC) and column adsorption kinetics were analysed. To test the hypothesis.

2. Materials and methods

2.1. Description of the experimental bench scale plant and experimental campaign

A bench scale column plant (Fig. 1) filled with biochar was built at the Water Resource Recovery Facility (WRRF) within Palermo University Campus Mannina et al., 2021b. Specifically, the column plant was constituted by three identical columns realized in polymethylmethacrylate, with an internal diameter of 5 cm and height of 20 cm, with a total volume of 0.39 L. To have a value in triplicate, the three columns worked in parallel with an individual feed pump. Each column was filled with 37 g of biochar obtained by pyrolysis at 880 °C of wood residues (a mixture of pine and eucalyptus at an equal ratio) from thinning.

Before its use, biochar (ø 2–5 mm) was washed three times with distilled water (200 g of biochar with 1.5 L) to remove particulate impurities and dried at 60 °C for 72 h. Then, according to Guo et al. [22], the biochar was pre-treated with hydrochloric acid (HCl) to

Table 1
Physical and chemical characteristics of the biochar before and after the treatment with 1 M hydrochloric acid.

Parameter	Units	Biochar	Biochar + HCl
Bulk density	g L^{-1}	126 ± 4	92 ± 3
Surface area	m^2 g^{-1}	227 ± 18	262 ± 12
Total pore volume	cm^3 g^{-1}	51 ± 4	71 ± 6
Maximum water retention	%	400 ± 18	442 ± 15
Soil reaction	pH	10 ± 0.6	8.1 ± 0.2
Electrical conductivity	dS m^{-1}	2 ± 0.3	1.3 ± 0.2
Moisture	%	6.7 ± 0.5	8.2 ± 0.7
Total limestone	%	2.7 ± 0.6	- -
Total carbon	%	72 ± 6	68 ± 4
Ashes to 550 C°	%	6.4 ± 0.4	5.2 ± 0.4
Molar ratio H:C	///	0.21 ± 0.03	0.41 ± 0.07
Total nitrogen (N)	%	0.29 ± 0.05	0.25 ± 0.02
Total phosphorus (P_2O_5)	g kg^{-1}	0.22 ± 0.04	0.19 ± 0.05
Total potassium (K_2O)	g kg^{-1}	4.0 ± 0.7	3.1 ± 0.6
Total calcium (CaO)	g kg^{-1}	11 ± 2	6 ± 1

6.5.

Table 2
Main chemical characteristics of treated real wastewater used to feed the columns filled with biochar for P removal.

Parameter	Symbol	Units	Average ± SD
Soluble COD	sCOD	mg L^{-1}	42.9 ± 26.4
Total Nitrogen	TN	mg L^{-1}	17.6 ± 5.6
Ammonium	NH_4–N	mg L^{-1}	5.5 ± 5.1
Phosphate	PO_4–P	mg L^{-1}	10.5 ± 2.1
Flow Rate	Q_{IN}	L h^{-1}	0.7-1.7-2.3
Escherichia Coli	EC	MPN 100 mL^{-1}	2.8 ± 6.2
Empty bed contact time	EBCT	min	26.5-10.6-7.6
Reaction	pH	–	6.9–7.7

remove carbonates and improve its adsorption efficiency. Precisely, 150 g of dried biochar was shaken for 12 h at 80 rpm with 1 M HCl solution (1:5 ratio, w:v). Finally, biochar was washed once with distilled water (1:2.5 ratio, w:v) and dried at 60 °C for 72 h (Table 1).

The biochar obtained was characterised by acquiring Fourier transform and attenuated total reflectance infrared (ATR-FTIR) spectra (i.e., absorbance versus wave number) with a PerkinElmer Spectrum Two FTIR spectrometer equipped with an attenuated total reflectance (ATR) device. The spectra were acquired to evaluate the main functional groups of the tested biochar. Approximately 1 mg of pulverised biochar was used to acquire spectra in the wavenumber range 3600-600 cm^{-1}, with a resolution of 4 cm^{-1} and 32 scans. According to Sharma et al. [23], this infrared spectral region is useful for characterising biochar's structural characteristics. In addition, as suggested by Zhou et al. [24], the infrared spectral region between 1190 and 600 cm^{-1} was monitored to assess P adsorption by biochar. Spectra were processed using PerkinElmer Spectrum software (version 10.5.1).

Biochar's zero charge point (pH_{pzc}) was determined with a pH meter (FiveEasy, Mettler Toledo Spa, Milan, Italy) equipped with a glass electrode. According to Nasiruddin et al. [25], the pH drift method described in Vaičiukyniene et al. (2020) was used. Sodium chloride (0.01 M) was used as the background electrolyte. Eight solutions with pH values ranging from 2 to 9 were prepared, adjusting the pH by adding small amounts of 0.5 M HCl or 0.5 M NaOH solutions. Then, 0.1 g of biochar was soaked with 40 mL of each solution and left to stand for 24 h at room temperature. The final pH of each solution was measured. The pH_{pzc} of the biochar was evaluated as follows: if the initial pH of the solution was equal to the final pH of the solution, then this was considered the pH_{pzc}, and the charge on the surface of the biochar was assumed to be zero (Vaičiukyniene et al., 2020). Cleaned quartz sand (ø 2–5 mm) sandwiched the biochar layer at the top and bottom to immobilize the biochar layer and enhance a uniform flow distribution over the cross-sectional area. The column plant was fed with real treated wastewater produced by a biological pilot plant treating real domestic wastewater equipped with an ultrafiltration membrane to remove pathogenic microorganisms [26]. The columns worked with an upward flow and the treated wastewater was fed into the columns using a peristaltic pump (Watson Marlow-Qdos 30 Universal).

Wastewater characteristics and main treatment features are reported in Table 2. The global duration of the experimental campaign was 90 days divided into three periods (namely, Period I, Period II and Period III, respectively). Each period was characterized by a different value of the feeding flow rate: 0.7, 1.7 and 2.3 L h^{-1}, respectively in Period I, Period II and Period III. The concentration of ions, acidity, and electrical conductivity in treated wastewater were measured at the inlet and outlet of the columns. Concerning the sampling frequency, samples were collected in the first 24 h of operation after 0.5, 1, 3, 5 and 24 h, respectively. Afterwards, samples were collected daily until the end of the experiment.

2.2. Analytical methods

Before being analysed by ion chromatography, samples were filtered through membrane syringe filters with a pore size of 0.45 μm

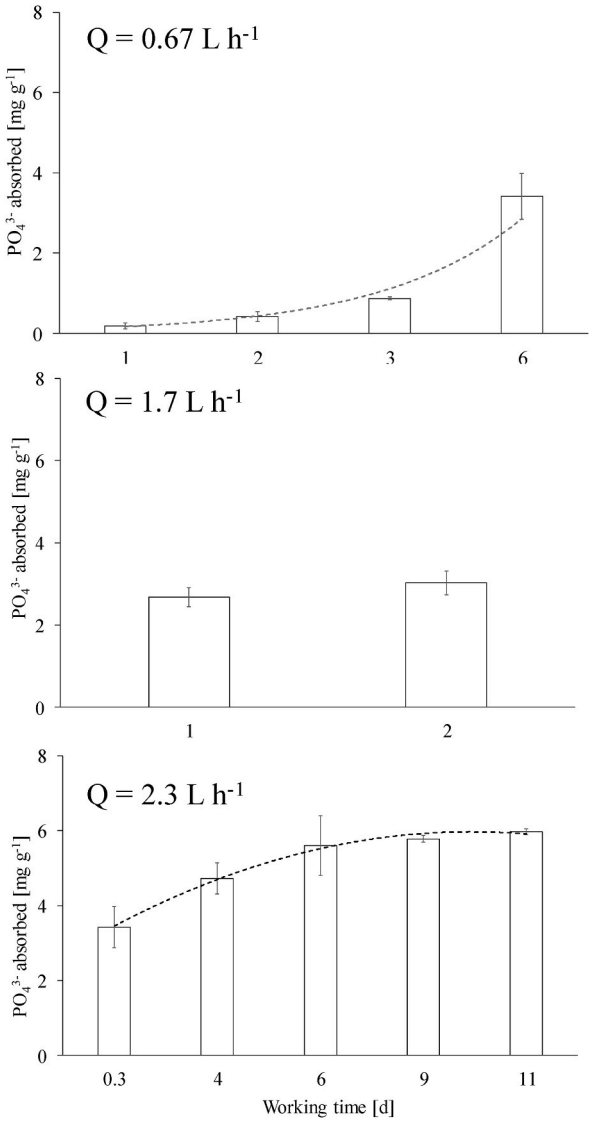

Fig. 2. Specific phosphate absorption rate during Period I (a), Period II (b) and Period III (c), respectively, with different influent loading rate (Q).

to remove any impurities and thus protect the analytical columns [27]. The concentration of fluoride (F^-), chloride (Cl^-), nitrite (NO_2^-), nitrate (NO_3^-), phosphate (PO_4^{3-}) and sulphate (SO_4^{2-}) was determined by Dionex Easion, Thermo Scientific Ionic chromatograph, with Dionex IonPac AS22 (4 × 250 mm) column. The used reagents were Dionex Anion Regenerant Concentrate, Thermo Scientific (72 mN Sulfuric Acid), Dionex AS22 Eluent Concentrate, Thermo Scientific (4.5 mM Sodium Carbonate and 1.4 mM Sodium Bicarbonate) for anion determination. The Ion Chromatograph was coupled with Autoanalyzer Dionex AS-DV, Thermo Scientific. The P exchange capacity (PEC) of the biochar was assessed as the ratio between the P adsorbed by biochar (mg g^{-1}) and the P fed to the system (mg L^{-1}). Acidity was measured by a pH meter (FiveEasy, Mettler Toledo S.p.a., Milan, Italy), whereas electrical conductivity (EC) was measured by a conductometer (HI5321, Hanna Instruments Italia S.r.l., Padua, Italy). The data reported for each period are the average values for the three columns.

2.3. Adsorption kinetics

The kinetics of PO_4^{3-} adsorption were evaluated by modelling experimental data from biochar packed column over the first 72-h. Ultrafiltered wastewater was fed into the column at a constant concentration of 10.5 ± 2.1 mg PO_4^{3-} L^{-1}, and the PO_4^{3-} concentration in the filtered wastewater was measured at 30, 45 min, 1 h, 1.5 h, 2 h, 3 h, 5 h, 24 h, 48 h, and 72 h. Data were analysed mathematically, applying both pseudo-first and pseudo-second order models. The pseudo-first order model (eq. (1)) Lagergren [28] assumes that the adsorption rate is solely dependent on the amount of PO_4^{3-} in contact with the biochar:

Table 3
A comparative studies reveling the application of biochar as an adsorbent in removal of phosphate from synthetic water/real wastewater.

Reference	Experiment types	Adsorbents	Wastewater types	Initial P concentration (mg L^{-1})	Temperature (°C)	pH	Duration (h)	Adsorption Capacity (mg g^{-1})
Jung et al. [12]	Batch	Electrochemically modified biochar calcium-alginate beads	Synthetic water	500	20	4.0	24	169.89
	Fixed-bed column	Electrochemically modified biochar calcium-alginate beads	Synthetic water	30	20	4.0	–	23.81–98.44
Huggins et al. [14]	Batch	Pristine biochar	Real brewery wastewater	18	20 ± 2	–	24	1.00
	Fixed-bed column	Pristine biochar	Real brewery wastewater	18	–	–	72	2.60
	Batch	Granular activated carbon (GAC)	Real brewery wastewater	18	20 ± 2	–	24	0.49
	Fixed-bed column	Granular activated carbon (GAC)	Real brewery wastewater	18	–	–	72	1.90
Present study	Fixed-bed column – Period I	Pristine biochar	Ultrafiltered real domestic wastewater	10.5 ± 2.1	25	6.9–7.7	24	0.19
	Fixed-bed column – Period I	Pristine biochar	Ultrafiltered real domestic wastewater	10.5 ± 2.1	25	6.9–7.7	144	3.41
	Fixed-bed column – Period II	Pristine biochar	Ultrafiltered real domestic wastewater	10.5 ± 2.1	25	6.9–7.7	24	2.70
	Fixed-bed column – Period III	Pristine biochar	Ultrafiltered real domestic wastewater	10.5 ± 2.1	25	6.9–7.7	7	3.43
	Fixed-bed column – Period III	Pristine biochar	Ultrafiltered real domestic wastewater	10.5 ± 2.1	25	6.9–7.7	144	6.00

$$q_t = q_e\left(1 - e^{-k_1 t}\right) \tag{1}$$

where q_t in mg PO_4^{3-} $g^{-1}$is the amount of PO_4^{3-} adsorbed by biochar at time t, q_e is the equilibrium adsorption capacity (mg $PO_4^{3-}g^{-1}$) and k_1 (h^{-1}) is the pseudo-first order monomodal constant. The latter is directly related to the adsorption rate of PO_4^{3-} by biochar. The higher is the k_1 the value, the faster the PO_4^{3-} adsorption rate.

The pseudo-second order model (eq. (2)) [29] assumes a chemisorption process, i.e. an adsorption process that involves a chemical reaction and that implies the formation of a covalent bond between the molecule and one or more atoms on the surface. In this scenario, the rate of adsorption depends on the adsorption capacity rather than the concentration of PO_4^{3-} in contact with the biochar Sahoo & Prelot, 2020.

$$q_t = \frac{k_2 q_{et}^2}{1 + k_2 qet} \tag{2}$$

where q_t (mg PO_4^{3-} g^{-1}) is the amount of PO_4^{3-} adsorbed at time t, q_e is the amount of PO_4^{3-} adsorbed at equilibrium (mg PO_4^{3-} g^{-1}), k_2 (h^{-1}) is the pseudo second order rate constant, and is constantly related to the energy of adsorption.

The basic assumptions of the Elovich model include two key points: first, that the activation energy increases with the duration of adsorption, and second, that the surface of the adsorbent exhibits heterogeneity. Although this model is widely used in modelling gas adsorption on solids, it is essentially empirical and lacks precise physical interpretations. Equation 3, formulated by Ref. [30], outlines the essence of the Elovich model.

$$qt = \frac{1}{b}\ \ln(1 + abt)$$

where q_t (mg PO_4^{3-} L^{-1}) is the amount of PO_4^{3-} adsorbed at time t. “a” Initial adsorption rate constant of the Elovich model (mg g^{-1} h^{-1}), “b” is the desorption rate constant of the Elovich model (mg g^{-1}).The performance of the different kinetic models was evaluated through the application of different statistical parameters, such as correlation coefficient (R^2), chi-square (χ^2), residual sum of squares error (SSE), and mean sum of squares error (MSE).The kinetics have been analysed using a user-friendly UI developed based on Excel ([31].

Table 4
Correlation analysis among anions concentration, pH and electrical conductivity (EC) determined on treated wastewater at the outlet of the columns at each period (Period I, Period II, Period III). *, $p < 0.05$; **, $p < 0.01$

Period I								
Variables	hours	pH	CE (dS m^{-1})	F^- (mg L^{-1})	Cl^- (mg L^{-1})	NO_2^- (mg L^{-1})	NO_3^- (mg L^{-1})	PO_4^{3-} (mg L^{-1})
pH	0.616*							
CE (dS m^{-1})	−0.585*	−0.968**						
F^- (mg L^{-1})	0.675*	0.333	−0.362					
Cl^- (mg L^{-1})	−0.734**	−0.903**	0.943**	−0.590*				
NO_2^- (mg L^{-1})	−0.359	0.091	−0.093	−0.437	−0.040			
NO_3^- (mg L^{-1})	0.417	0.811**	−0.874**	0.463	−0.793**	−0.138		
PO_4^{3-} (mg L^{-1})	−0.405	−0.627*	0.603*	−0.076	0.625*	−0.472	−0.211	
SO_4^{2-} (mg L^{-1})	0.294	−0.443	0.482	0.204	0.231	−0.203	−0.678*	−0.071
Period II								
Variables	hours	pH	CE (dS m^{-1})	F^- (mg L^{-1})	Cl^- (mg L^{-1})	NO_2^- (mg L^{-1})	NO_3^- (mg L^{-1})	PO_4^{3-} (mg L^{-1})
pH	0.763							
CE (dS m^{-1})	−0.569	−0.925**						
F^- (mg L^{-1})	−0.453	0.089	−0.294					
Cl^- (mg L^{-1})	−0.555	0.081	−0.245	0.880*				
NO_2^- (mg L^{-1})	0.623	0.333	−0.321	−0.028	−0.458			
NO_3^- (mg L^{-1})	0.679	0.066	0.148	−0.866*	−0.981**	0.499		
PO_4^{3-} (mg L^{-1})	−0.795	−0.954**	0.873*	−0.116	−0.049	−0.483	−0.100	
SO_4^{2-} (mg L^{-1})	−0.751	−0.397	0.063	0.543	0.505	−0.321	−0.638	0.511
Period III								
Variables	hours	pH	EC (dS m^{-1})	F^- (mg L^{-1})	Cl^- (mg L^{-1})	NO_2^- (mg L^{-1})	NO_3^- (mg L^{-1})	PO_4^{3-} (mg L^{-1})
pH	0.421							
EC (dS m^{-1})	−0.472	−0.830**						
F^- (mg L^{-1})	0.370	0.743*	−0.829**					
Cl^- (mg L^{-1})	0.250	0.005	0.108	−0.474				
NO_2^- (mg L^{-1})								
NO_3^- (mg L^{-1})	−0.742*	−0.573	0.400	−0.625	0.136			
PO_4^{3-} (mg L^{-1})	−0.823**	−0.730*	0.660*	−0.759*	0.124		0.942**	
SO_4^{2-} (mg L^{-1})	0.479	0.200	−0.272	−0.206	0.847**		0.096	−0.073

2.4. Correlation analysis

For each period, correlation analysis among anions concentration, pH, and EC was determined using SPSS 13.0 on treated wastewater at the outlet of the columns.

3. Results and discussion

FTIR spectra of the HCl-treated biochar before and after phosphate adsorption were similar (Fig. S1). Peaks refer to functional groups similar to woody matrix biochar [32,33]. The peak near 1100 cm^{-1} can be assigned to P–O stretching vibration of the PO_4^{3-} group. Such results align with those of Xia et al. [34], who observed that P was successfully adsorbed by biochar obtained at 400 °C from tobacco sticks.

Fig. 2 shows the PO_4^{3-} specific adsorption rate during Period I (Fig. 2a), Period II (Fig. 2b) and Period III (Fig. 2c), respectively. The specific PO_4^{3-} adsorption rate of biochar with a working influent flow rate of 0.67 L h^{-1} for each column followed an exponential trend in agreement with previous studies (e.g. Ref. [14]).

Indeed, after one working day, the amount of PO_4^{3-} adsorbed by biochar was 0.19 mg g^{-1}, while on day 6, it reached the value of 3.41 mg g^{-1} (Table 3). The achieved P adsorption was generally lower than reported in the literature (Table 3). Indeed, Zhong et al. [35] found an adsorption capacity of 9.8, 18.8, and 23.3 mg g^{-1} in batch experiments carried out with coconut shell biochar/pristine biochar at 25, 35, and 45 °C, respectively, with PO_4^{3-} concentration of 100 mg L^{-1} (Table 3). These results can be likely related to the higher PO_4^{3-} concentration in their initial solution and the lower biochar size (<1 mm), which provided a higher contact surface. Indeed, in the current study, the initial PO_4^{3-} concentration was 10.5 ± 2.1 mg L^{-1} and the biochar particle size was 2–5 mm.

Therefore, due to the low adsorption rate at the beginning of the experiment, likely due to the low phosphorus loading rate because of the low influent flow rate (0.67 L h^{-1}), the influent flow was increased up to 1.7 L h^{-1} (Period II). Following such an increase (Fig. 2b; Period II), a significantly higher amount of PO_4^{3-} was adsorbed by biochar after just one day of work compared to that achieved in Period I. Indeed, it was noticed, after one day of operation, an increase from 0.19 to 2.7 mg PO_4^{3-} g^{-1} biochar, thus highlighting that the increase of the influent flow, and consequently the increase of P loading rate, promoted an overall increase of PO_4^{3-} adsorption at the beginning of experiments. Nevertheless, after two days of work, a very moderate increase in PO_4^{-3} adsorption was noticed, close to only 10 % compared to the previous day. Therefore, the influent flow rate was decided to increase to 2.3 L h^{-1} (Period III). In Period III, after only 7 h of work(~0.3 day) the adsorbed PO_4^{3-} was 3.43 mg g^{-1} of biochar, thus confirming that a

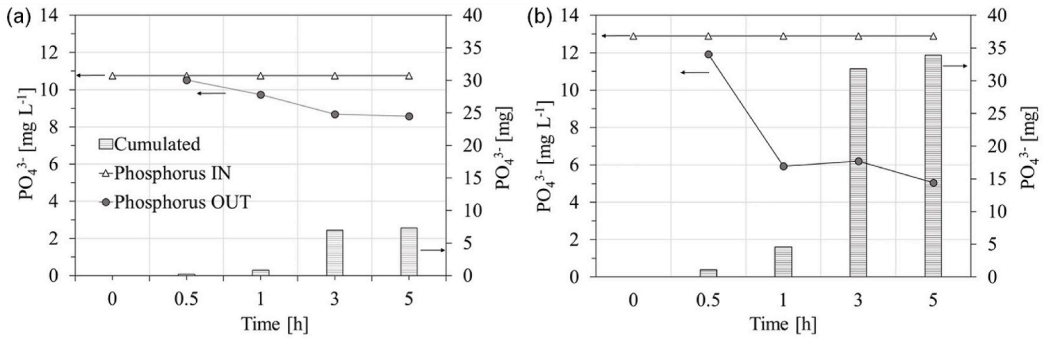

Fig. 3. Influent and effluent PO_4^{3-} concentrations and PO_4^{3-} absorbed after 5 h in Period II (a) and Period III (b), respectively.

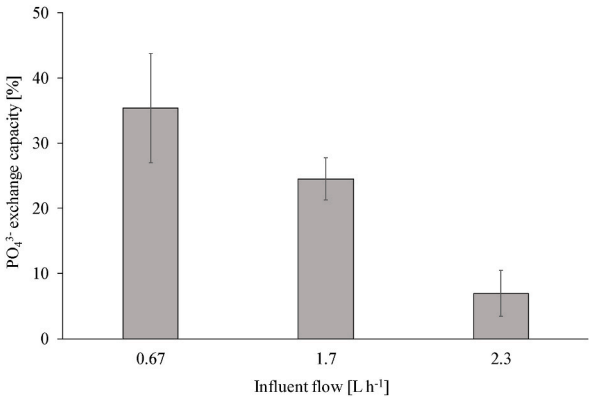

Fig. 4. Phosphorus exchange capacity (PEC) *vs* the influent flow rate.

further increase of influent P loading rate enhanced the recovery of P onto biochar. Afterwards, an almost linear increase in PO_4^{3-} adsorption up to day 6 was observed and the adsorption capacity showed an asymptotic trend, reaching a maximum value of 6 mg g^{-1}. The increase of PO_4^{3-} adsorbed with the increase of the influent flow rate disagrees with the literature [12]. Indeed, Jung and co-workers, investigating the effect of flow rate on PO_4^{3-} adsorption by changing the influent flow rate between 2.5, 5.9- and 7.5-mL min^{-1}, found that the breakthrough generally occurred faster with a higher flow rate, indicating a lower saturation duration. Hence, PO_4^{3-} adsorption on biochar reduces with increased flow rate, which may be caused by the solute not having enough time to settle and contact the accessible binding sites for the PO_4^{3-} on the biochar surface.

Moreover, EC and pH are important in determining the amount of PO_4^{3-} adsorbed by biochar. At each sampling period, PO_4^{3-} determined on the treated wastewater at the outlet of the columns was positively correlated with EC and inversely pH (Table 4). The positive correlation with EC is reasonable and indicates that, by increasing salts concentration, the concentration of PO_4^{3-} in the effluent increases probably due to an excessive presence of salts in the influent and the inability of biochar to adsorb all soluble salts. The form of PO_4^{3-} in aqueous solution depends on the pH [36]. Considering that the pH of the treated wastewater ranged from 6.9 to 7.7, among the four phosphate forms (H_3PO_4, $H_2PO_4^-$, HPO_4^{2-}, and PO_4^{3-}), $H_2PO_4^-$ and HPO_4^{2-} were the dominant species. Thus, the inverse relationship with pH may be ascribed to the competition of OH^- for the adsorption sites with PO_4^{3-} in solution, resulting in a decrease in phosphate adsorption capacity [37], and to PO_4^{3-} precipitation with Ca^{2+} and Mg^{2+} to form less soluble salts [38]. Such results agreed with those of the pH_{pzc}. The pH_{pzc} (Fig. S2) of biochar is fundamental to foresee if biochar in contact with aqueous solution may absorb phosphate. Indeed, when pH of the solution is lower than the biochar's pH_{pzc}, the biochar's positively charged surface favours the adsorption of anionic P species. Conversely, when pH is higher than the pH_{pzc}, functional groups are protonated, so a lower amount of P is adsorbed. The pH_{pzc} of biochar treated with HCl was 6.7 (Fig. S2). Thus, by relating the pH of treated wastewater and pHpzc of biochar, the low amount of P adsorbed by biochar can be easily explained.

To stress the different adsorption behaviour under different loading rates, Fig. 3 shows the trend of PO_4^{3-} concentration at the inlet and outlet of the columns as well as the cumulated PO_4^{3-} adsorbed during the first 5 h of flushing, respectively, in Period II (Fig. 3a) and Period III (Fig. 3b).

The higher PO_4^{3-} adsorption in Period III compared to Period II is likely due to the higher P loading rate to the columns. Indeed, in Period II, only 15.3 mg PO_4^{3-} were adsorbed by biochar after 5 h of work; in contrast, in Period III, after the same duration, biochar adsorbed 77 mg PO_4^{3-} thus suggesting that the overall mass of adsorbed P on the biochar surface is dependent on the influent flow. It is to be noted that, during the 5 h, the phosphate concentration decreased over time. Indeed, since fresh adsorbent was used at the beginning of each experiment, one would expect the outlet phosphate concentration to be essentially zero at the start and increase over

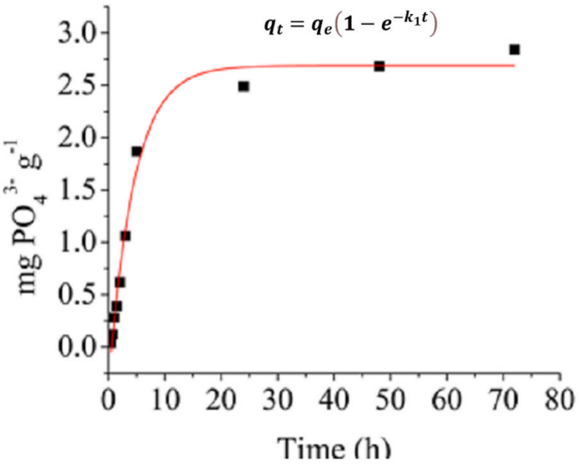

Fig. 5. Monomodal pseudo-first adsorption kinetics by biochar in period III.

Table 5
Parameter values obtained from applying pseudo-first, pseudo-second order and Elovich kinetic models to experimental data of phosphate adsorption by biochar in bench scale columns. R^2, correlation coefficient; χ^2, chi-square, SSE, residual sum of squares error, and MSE, mean sum of squares error.

Pseudo first-order model	R^2	χ^2	SSE	MSE	k_1 ($\frac{1}{h}$)	q_e (mg g^{-1})
	0.968	0.489	0.314	0.031	0.16	2.7
Pseudo-second order model	R^2	χ^2	SSE	MSE	k_2 ($\frac{1}{h}$)	q_e (mg g^{-1})
	0.959	0.632	0.412	0.041	0.05	3.1
Elovich model	R^2	χ^2	SSE	MSE	a (mg g^{-1} h^{-1})	b (mg g^{-1})
	0.929	0.933	0.728	0.072	0.672	1.39

time due to the saturation of the sorbent. Such unexpected behaviour can be attributed to the need for further cleaning of biochar pores and surfaces from dust and other dirtiness Guo et al., 2019. To highlight the effect of hydraulic loading rate on the adsorption performance of biochar, for each period, the PEC was computed as the ratio between the PO_4^{3-} adsorbed by biochar and the PO_4^{3-} fed to the system in the same working time (Fig. 4).

As noticeable from Fig. 4, despite the present study, the highest amount of recovered PO_4^{3-} was achieved in Period III, with the highest influent flow rate; in terms of PO_4^{3-} recovery, the efficiency referred to the influent loading rate is inversely proportional to the influent flow rate. Indeed, the PEC values were equal to 35, 24.5 and 8.9 % for flow rates of 0.67, 1.7 and 2.3 L h^{-1}, respectively. This result agrees with the results achieved in the study of Jung et al. [12], where a reduction of PO43钓 adsorption performance was found with the increasing flow rate. According to Chu [39] and Salman et al. [40], this phenomenon might be related to the low residence time of the solute, which is insufficient to provide the proper contact between PO_4^{3-} and the binding sites at higher flow rates. Similarly, Kizito et al. [41] investigated ammonium adsorption in biochar columns by varying the flow rate from 15 to 25 mL min^{-1} and found higher NH_4–N removal at the lowest flow rate. This result was attributed by Kizito and co-workers to the reduced residence time of the solute in the sorption bed at a higher flow rate.

Therefore, if the aim is PO_4^{3-} recover to prevent eutrophication of water bodies, results suggest working with lower flow rates for a higher duration. In contrast, if the aim is to maximize PO_4^{3-} recovery in view of using the enriched biochar as a slow-release fertilizer, the suggestion is to apply higher flow rates to quickly adsorb P.

Adsorption kinetic studies of PO_4^{3-} only pertain to Period III, which yielded the highest PO_4^{3-} adsorption onto biochar. The amounts of PO_4^{3-} adsorbed as a function of contact time are reported in Fig. 5. Adsorption of PO_4^{3-} was fast during the first 5 h and then slowed down.

The pseudo-first-order kinetic model returned higher R^2 values and lower χ^2, SSE and MSEvalues than the pseudo-second-order and Elovich kinetic models (Table 5), thus indicating a better fit of the former model (Fig. 5). Such results suggest that the adsorption rate is solely dependent on the amount of PO_4^{3-} in contact with the biochar (physiosorption mechanism; [28,31]).

4. Conclusions

Biochar was tested as an adsorbent material to recover P from real wastewater treated with an advanced membrane system. The results highlighted an effective P recovery with the highest amount of P adsorption with the increase of flow rate (namely, 3.43 mg P g^{-1} at a flow rate of 2.3 L h^{-1}). Nevertheless, the P adsorption capacity achieved in this study was generally lower compared to previous findings; these results could be likely due to the size of the biochar used and the treated water's features. Future research should investigate biochar's adsorption ability, characterized by smaller size (higher contact surface) and water with higher P concentrations. On the other hand, the highest PEC efficiency (i.e., 35 %) was found at the lowest investigated flow rate. This aspect is

relevant since, in this way, it is possible to pursue P recovery in view of preventing at the same time water body's eutrophication. Pseudo-first-order model best approximated the adsorption kinetics, thus suggesting that the adsorption of phosphate by biochar depends on its concentrations (i.e. physiosorption mechanism).

CRediT authorship contribution statement

Sofia Maria Muscarella: Investigation. **Daniele Di Trapani:** Data curation, Conceptualization. **Vito Armando Laudicina:** Validation, Supervision, Software, Conceptualization. **Giorgio Mannina:** Writing – original draft, Methodology, Investigation, Funding acquisition, Data curation, Conceptualization.

Declaration of competing interest

The authors declare that they have no known competing financial interests or personal relationships that could have appeared to influence the work reported in this paper.

Acknowledgements

This work was funded by the project "Achieving wider uptake of water-smart solutions—WIDER UPTAKE" (grant agreement number: 869283) financed by the European Union's Horizon 2020 Research and Innovation Programme, in which Giorgio Mannina, is the principal investigator for the University of Palermo. The Unipa project website can be found at: https://wideruptake.unipa.it/

Appendix A. Supplementary data

Supplementary data to this article can be found online at https://doi.org/10.1016/j.heliyon.2024.e34659.

References

[1] M.M. Thant Zin, D.J. Kim, Simultaneous recovery of phosphorus and nitrogen from sewage sludge ash and food wastewater as struvite by Mg-biochar, J. Hazard Mater. 403 (August 2020) (2021) 123704, https://doi.org/10.1016/j.jhazmat.2020.123704.
[2] P. Cornel, C.J.W.S. Schaum, Phosphorus recovery from wastewater: needs, technologies and costs, Water Sci. Technol. 59 (6) (2009) 1069–1076.
[3] J.T. Bunce, E. Ndam, I.D. Ofiteru, A. Moore, D.W. Graham, A review of phosphorus removal technologies and their applicability to small-scale domestic wastewater treatment systems, Front. Environ. Sci. 6 (2018), https://doi.org/10.3389/fenvs.2018.00008.
[4] H.M. Azam, S.T. Alam, M. Hasan, D.D.S. Yameogo, A.D. Kannan, A. Rahman, M.J. Kwon, Phosphorous in the environment: characteristics with distribution and effects, removal mechanisms, treatment technologies, and factors affecting recovery as minerals in natural and engineered systems, Environ. Sci. Pollut. Control Ser. 26 (20) (2019) 20183–20207, https://doi.org/10.1007/s11356-019-04732-y.
[5] A.V. Baskar, N. Bolan, S.A. Hoang, P. Sooriyakumar, M. Kumar, L. Singh, T. Jasemizad, L.P. Padhye, G. Singh, A. Vinu, B. Sarkar, M.B. Kirkham, J. Rinklebe, S. Wang, H. Wang, R. Balasubramanian, K.H.M. Siddique, Recovery, regeneration and sustainable management of spent adsorbents from wastewater treatment streams: a review, Sci. Total Environ. 822 (2022) 153555, https://doi.org/10.1016/j.scitotenv.2022.153555.
[6] S. Ambika, M. Kumar, L. Pisharody, M. Malhotra, G. Kumar, V. Sreedharan, L. Singh, P.V. Nidheesh, A. Bhatnagar, Modified biochar as a green adsorbent for removal of hexavalent chromium from various environmental matrices: mechanisms, methods, and prospects, Chem. Eng. J. 439 (2022) 135716, https://doi.org/10.1016/j.cej.2022.135716.
[7] M. Marcińczyk, Y.S. Ok, P. Oleszczuk, From waste to fertilizer: nutrient recovery from wastewater by pristine and engineered biochars, Chemosphere 306 (2022) 135310, https://doi.org/10.1016/j.chemosphere.2022.135310.
[8] K. Abhishek, A. Shrivastava, V. Vimal, A.K. Gupta, S.K. Bhujbal, J.K. Biswas, L. Singh, P. Ghosh, A. Pandey, P. Sharma, M. Kumar, Biochar application for greenhouse gas mitigation, contaminants immobilization and soil fertility enhancement: a state-of-the-art review, Sci. Total Environ. 853 (2022) 158562, https://doi.org/10.1016/j.scitotenv.2022.158562.
[9] N. Bolan, S.A. Hoang, J. Beiyuan, S. Gupta, D. Hou, A. Karakoti, S. Joseph, S. Jung, K.-H. Kim, M.B. Kirkham, H.W. Kua, M. Kumar, E.E. Kwon, Y.S. Ok, V. Perera, J. Rinklebe, S.M. Shaheen, B. Sarkar, A.K. Sarmah, L. Van Zwieten, Multifunctional applications of biochar beyond carbon storage, Int. Mater. Rev. 67 (2) (2022) 150–200, https://doi.org/10.1080/09506608.2021.1922047.
[10] A. Nicosia, V. Pampalone, V. Ferro, Effects of biochar addition on rill flow resistance, Water (Switzerland) 13 (21) (2021), https://doi.org/10.3390/w13213036.
[11] I.W. Almanassra, G. Mckay, V. Kochkodan, M. Ali Atieh, T. Al-Ansari, A state of the art review on phosphate removal from water by biochars, Chem. Eng. J. 409 (2021) 128211, https://doi.org/10.1016/j.cej.2020.128211.
[12] K.W. Jung, T.U. Jeong, J.W. Choi, K.H. Ahn, S.H. Lee, Adsorption of phosphate from aqueous solution using electrochemically modified biochar calcium-alginate beads: batch and fixed-bed column performance, Bioresour. Technol. 244 (July) (2017) 23–32, https://doi.org/10.1016/j.biortech.2017.07.133.
[13] Y. Zheng, B. Wang, A.E. Wester, J. Chen, F. He, H. Chen, B. Gao, Reclaiming phosphorus from secondary treated municipal wastewater with engineered biochar, Chem. Eng. J. 362 (2019) 460–468, https://doi.org/10.1016/j.cej.2019.01.036.
[14] T.M. Huggins, A. Haeger, J.C. Biffinger, Z.J. Ren, Granular biochar compared with activated carbon for wastewater treatment and resource recovery, Water Res. 94 (2016) 225–232, https://doi.org/10.1016/j.watres.2016.02.059.
[15] Y.-P. Gong, Z.-Y. Ni, Z.-Z. Xiong, L.-H. Cheng, X.-H. Xu, Phosphate and ammonium adsorption of the modified biochar based on Phragmites australis after phytoremediation, Environ. Sci. Pollut. Res. Int. 24 (9) (2017) 8326–8335, https://doi.org/10.1007/s11356-017-8499-2.
[16] M. Peter-Varbanets, C. Zurbrügg, C. Swartz, W. Pronk, Decentralized systems for potable water and the potential of membrane technology, Water Res. 43 (2) (2009) 245–265, https://doi.org/10.1016/j.watres.2008.10.030.
[17] T. Nguyen, Adsorption of Phosphorus from Wastewater onto Biochar: Batch and Fixed-Bed Column Studies, 2015.
[18] T.P. Tran, T.P. Nguyen, X.C. Nguyen, X.H. Nguyen, T.H. Nguyen, T.N. Nguyen, D.D. Nguyen, Adsorptive removal of phosphate from aqueous solutions using low-cost modified biochar-packed column: effect of operational parameters and kinetic study, Chemosphere 309 (2022) 136628.
[19] M.B. Shakoor, Z.-L. Ye, S. Chen, Engineered biochars for recovering phosphate and ammonium from wastewater: a review, Sci. Total Environ. 779 (2021) 146240, https://doi.org/10.1016/j.scitotenv.2021.146240.

[20] D. Jiang, B. Chu, Y. Amano, M. Machida, Removal and recovery of phosphate from water by Mg-laden biochar: batch and column studies, Colloids Surf. A Physicochem. Eng. Asp. 558 (September) (2018) 429–437, https://doi.org/10.1016/j.colsurfa.2018.09.016.
[21] Y. Wang, L.P. Qiu, M.F. Hu, Magnesium ammonium phosphate crystallization: a possible way for recovery of phosphorus from wastewater, IOP Conf. Ser. Mater. Sci. Eng. 392 (3) (2018), https://doi.org/10.1088/1757-899X/392/3/032032.
[22] J. Guo, S. Jiang, Y. Pang, Rice straw biochar modified by aluminum chloride enhances the dewatering of the sludge from municipal sewage treatment plant, Sci. Total Environ. 654 (2019) 338–344, https://doi.org/10.1016/j.scitotenv.2018.10.429.
[23] R.K. Sharma, J.B. Wooten, V.L. Baliga, X. Lin, W. Geoffrey Chan, M.R. Hajaligol, Characterization of chars from pyrolysis of lignin, Fuel 83 (11) (2004) 1469–1482, https://doi.org/10.1016/j.fuel.2003.11.015.
[24] Y. Zhou, A. Selvam, J.W.C. Wong, Chinese medicinal herbal residues as a bulking agent for food waste composting, Bioresour. Technol. 249 (2018) 182–188, https://doi.org/10.1016/j.biortech.2017.09.212. September 2017.
[25] M. Nasiruddin Khan, A. Sarwar, Determination of points of zero charge of natural and treated adsorbents, Surf. Rev. Lett. 14 (3) (2007) 461–469.
[26] A. Cosenza, H. Gulhan, C.M. Maida, G. Mannina, Nutrient recovery from wastewater treatment by ultrafiltration membrane for water reuse in view of a circular economy perspective, Bioresour. Technol. 363 (2022) 127929, https://doi.org/10.1016/j.biortech.2022.127929.
[27] R. Michalski, Ion chromatography applications in wastewater analysis, Separations 5 (1) (2018), https://doi.org/10.3390/separations5010016.
[28] S. Lagergren, About the theory of so-called adsorption of soluble substances. K. Sven, Vetenskapsakad. Handl. 24 (1898) 1–39.
[29] Y.S. Ho, D.A.J. Wase, C.F. Forster, Removal of lead ions from aqueous solution using sphagnum moss peat as adsorbent, WaterSA 22 (1996) 219–224.
[30] S.Y. Elovich, O.G. Larinov, Theory of adsorption from solutions of non-electrolytes on solid (I) equation adsorption from solutions and the analysis of its simplest form, (II) verification of the equation of adsorption isotherm from solutions, Izv. Akad. Nauk. SSSR, Otd. Khim. Nauk. 2 (1962) 209–216.
[31] J. Wang, X. Guo, Adsorption kinetic models: physical meanings, applications, and solving methods, J. Hazard Mater. 390 (2020) 122156.
[32] Y. Liu, Z. He, M. Uchimiya, Comparison of biochar formation from various agricultural by-products using FTIR spectroscopy, Mod. Appl. Sci. 9 (4) (2015) 246–253, https://doi.org/10.5539/mas.v9n4p246.
[33] J.O. Eduah, E.K. Nartey, M.K. Abekoe, S.W. Henriksen, M.N. Andersen, Mechanism of orthophosphate (PO4-P) adsorption onto different biochars, Environ. Technol. Innov. 17 (2020) 100572.
[34] S. Xia, S. Liang, Y. Qin, W. Chen, B. Xue, B. Zhang, G. Xu, Significant improvement of adsorption for phosphate removal by lanthanum-loaded biochar, ACS Omega 8 (28) (2023) 24853–24864.
[35] Z. Zhong, G. Yu, W. Mo, C. Zhang, H. Huang, S. Li, M. Gao, X. Lu, B. Zhang, H. Zhu, Enhanced phosphate sequestration by Fe(III) modified biochar derived from coconut shell, RSC Adv. 9 (18) (2019) 10425–10436, https://doi.org/10.1039/c8ra10400j.
[36] D.J. Greenland, The Chemistry of Soil Processes, New India Publishing Agency, 2015.
[37] F. Yang, S. Zhang, Y. Sun, D.C.W. Tsang, K. Cheng, Y.S. Ok, Assembling biochar with various layered double hydroxides for enhancement of phosphorus recovery, J. Hazard Mater. 365 (2019) 665–673, https://doi.org/10.1016/j.jhazmat.2018.11.047.
[38] K. Vikrant, K.-H. Kim, Y.S. Ok, D.C.W. Tsang, Y.F. Tsang, B.S. Giri, R.S. Singh, Engineered/designer biochar for the removal of phosphate in water and wastewater, Sci. Total Environ. 616–617 (2018) 1242–1260, https://doi.org/10.1016/j.scitotenv.2017.10.193.
[39] K.H. Chu, Fixed bed sorption: setting the record straight on the Bohart-Adams and Thomas models, J. Hazard Mater. 177 (1–3) (2010) 1006–1012, https://doi.org/10.1016/j.jhazmat.2010.01.019.
[40] J.M. Salman, V.O. Njoku, B.H. Hameed, Batch and fixed-bed adsorption of 2,4-dichlorophenoxyacetic acid onto oil palm frond activated carbon, Chem. Eng. J. 174 (1) (2011) 33–40, https://doi.org/10.1016/j.cej.2011.08.024.
[41] S. Kizito, H. Luo, S. Wu, Z. Ajmal, T. Lv, R. Dong, Phosphate recovery from liquid fraction of anaerobic digestate using four slow pyrolyzed biochars: dynamics of adsorption, desorption and regeneration, J. Environ. Manag. 201 (2017) 260–267, https://doi.org/10.1016/j.jenvman.2017.06.057.